The Astrophysical Journal, 856:47 (6pp), 2018 March 20 https://doi.org/10.3847/1538-4357/aab0a4

Merger of Multiple Accreting Black Holes Concordant with Gravitational-wave Events

Hiromichi Tagawa[1,2] and Masayuki Umemura[3]
[1] Institute of Physics, Eötvös University, Pázmány P.s., Budapest, 1117, Hungary; htagawa@caesar.elte.hu
[2] National Astronomical Observatory of Japan, 2-21-1 Osawa, Mitaka, Tokyo 181-8588, Japan
[3] Center for Computational Sciences, University of Tsukuba, Tsukuba, Ibaraki 305-8577, Japan
Received 2017 July 10; revised 2018 February 5; accepted 2018 February 16; published 2018 March 23

Abstract

Recently, the advanced Laser Interferometer Gravitational-Wave Observatory (aLIGO) has detected black hole (BH) merger events, most of which are sourced by BHs more massive than 30 $M_{\odot}$. Especially, the observation of GW170104 suggests dynamically assembled binaries favoring a distribution of misaligned spins. It has been argued that mergers of unassociated BHs can be engendered through a chance meeting in a multiple BH system under gas-rich environments. In this paper, we consider the merger of unassociated BHs, concordant with the massive BH merger events. To that end, we simulate a multiple BH system with a post-Newtonian N-body code incorporating gas accretion and general relativistic effects. As a result, we find that gas dynamical friction effectively promotes a three-body interaction of BHs in dense gas of $n_{\rm gas} \gtrsim 10^6$ cm^{-3}, so that BH mergers can take place within 30 Myr. This scenario predicts an isotropic distribution of spin tilts. In the concordant models with GW150914, the masses of seed BHs are required to be $\gtrsim 25\,M_{\odot}$. The potential sites of such chance meeting BH mergers are active galactic nucleus (AGN) disks and dense interstellar clouds. Assuming the LIGO O1, we roughly estimate the event rates for PopI BHs and PopIII BHs in AGN disks to be $\simeq$1–2 yr^{-1} and $\simeq$1 yr^{-1}, respectively. Multiple episodes of AGNs may enhance the rates by roughly an order of magnitude. For massive PopI BHs in dense interstellar clouds the rate is $\simeq$0.02 yr^{-1}. Hence, high-density AGN disks are a more plausible site for mergers of chance meeting BHs.

Key words: galaxies: active – gravitational waves – ISM: clouds – methods: numerical – stars: black holes – stars: Population III

1. Introduction

Recently, gravitational-wave (GW) emission associated with black hole (BH) mergers has been detected by the advanced Laser Interferometer Gravitational-Wave Observatory (aLIGO) in the events of GW150914 (Abbott et al. 2016a), GW151226 (Abbott et al. 2016b), GW170104 (Abbott et al. 2017a), GW170608 (Abbott et al. 2017b), and GW170814 (Abbott et al. 2017c). Excepting the GW151226 and GW170608 events, the BH pair in each event includes a BH more massive than 30 $M_{\odot}$. Abbott et al. (2016c) argued that such massive BHs are unlikely to originate in metal-rich stars owing to mass loss from stellar wind. As models for the BH merger events, several binary evolution scenarios have been proposed. They include a binary of metal-free or low-metallicity stars accompanied by mass transfer or common envelope ejection (e.g., Kinugawa et al. 2014; Belczynski et al. 2016), binary evolution in a tidally distorted field (e.g., de Mink & Mandel 2016), binary evolution driven by fallback accretion (Tagawa et al. 2018), and dynamical interaction in dense stellar clusters (e.g., O'Leary et al. 2009; Samsing et al. 2014; Rodriguez et al. 2016). Also, BH binaries may be hardened within gas-rich environments (Escala et al. 2004; Chapon et al. 2013), especially in active galactic nucleus (AGN) disks (Kocsis et al. 2011; McKernan et al. 2012, 2014, 2017; Bartos et al. 2017; Stone et al. 2017). McKernan et al. (2012, 2014) predicted the occurrence of intermediate BH mergers originating in AGN disks. McKernan et al. (2017) also considered binary formation of unassociated BHs through angular momentum exchange. Baruteau et al. (2011) investigated inward migration of massive stellar binaries hardened whitin a dense gaseous disk in the Galactic center.

GW observations can provide information about component spins through measurements of an effective inspiral spin parameter, $\chi_{\rm eff}$, which can potentially be used to distinguish different formation channels. Isolated binary evolution does not result in a significant spin misalignment, since mass transfer and tides align spins with the orbital angular momentum. The GW170104 event exhibits $\chi_{\rm eff} = -0.12^{+0.21}_{-0.30}$, which disfavors spin configurations with both component spins positively aligned with the orbital angular momentum (Abbott et al. 2017a), although the less massive BH merger in GW151226 has a preference for spins with positive projections along the orbital angular momentum (Abbott et al. 2016b). The observation of GW170104 hints toward dynamically assembled binaries favoring a distribution of misaligned spins rather than near orbit-aligned spins. Recently, Tagawa et al. (2015, 2016) proposed mergers of unassociated BHs through a chance meeting in gas-rich environments, without making a priori assumptions of a BH binary. They have demonstrated that a multiple stellar-mass BH system embedded in dense gas can engender mergers of BHs through gas dynamical friction and three-body interaction, which predicts an isotropic distribution of spin tilts.

In this paper, we consider BH mergers by chance meetings in a multiple BH system, especially focusing on the massive BH merger events (GW150914, GW170104, and GW170814). Favorable gas-rich environments for BH mergers are provided in nuclear regions of galaxies which have a density of $n_{\rm gas} \gtrsim 10^7$ cm^{-3} at $\lesssim$1 pc (Goodman 2003; Namekata &

Umemura 2016). Another possible site is dense interstellar cloud cores of $n_{\rm gas} = 10^{5-7}$ cm^{-3} (Bergin et al. 1996; Stahler 2010), or interstellar clouds of $n_{\rm gas} < 10^5$ cm^{-3} (Spitzer 1978). Simulations are performed with a highly accurate post-Newtonian N-body code, where general relativistic effects such as the pericenter shift and GW emission are taken into consideration. In these simulations, the effects of gas dynamical friction and Hoyle–Lyttleton mass accretion by ambient gas are incorporated. Changing initial masses of BHs, ambient gas density, and distributions of BHs, we derive the range of BH mass that is concordant with the GW events, and thereby assess the mass of accreting gas before mergers. Also, we roughly estimate the event rates of such BH mergers both in galactic centers and in dense interstellar clouds.

2. Post-Newtonian N-body Simulations

2.1. Numerical Scheme

A detailed description of the numerical schemes is given in Tagawa et al. (2016). The equations of motion are integrated using a fourth-order Hermite scheme (Makino & Aarseth 1992). Our simulations incorporate the effects of gas dynamical friction and gas accretion onto BHs. The general relativistic effects are dealt with a post-Newtonian prescription up to a 2.5PN term (Kupi et al. 2006), where the 1 PN and 2 PN terms correspond to the pericenter shift, and the 2.5PN term to GW emission.

2.2. Setup of Simulations

The key parameters in our simulations are initial BH mass (m_0), initial typical extension of BH distributions ($r_{\rm typ}$), ambient gas number density ($n_{\rm gas}$), and accretion efficiency (ϵ). We set the gas accretion rate of each BH to be the accretion efficiency ($\epsilon \leqslant 1$) times the Hoyle–Lyttleton accretion rate ($\dot{m}_{\rm HL}$), i.e.,

$$\dot{m}_i = \epsilon \dot{m}_{{\rm HL},i} = \epsilon \frac{4\pi G^2 m_{\rm H} n_{\rm gas} m_i^2}{(c_{\rm s}^2 + v_i^2)^{3/2}}, \quad (1)$$

where v_i is the velocity of ith BH, $c_{\rm s}$ is the sound speed, G is the Gravitational constant, and $m_{\rm H}$ is the hydrogen mass. The effect of radiation pressure on Hoyle–Lyttleton accretion (Watarai et al. 2000; Hanamoto et al. 2001) is incorporated as in Tagawa et al. (2016). This gas accretion prescription allows super-Eddington accretion, which is verified in spherical symmetric systems (e.g., Inayoshi et al. 2016). We consider multiple BHs that are embedded in high-density gas, e.g., in galactic nuclear regions of $\lesssim$1 pc or in dense interstellar clouds. Then, typical extensions of BH distributions at an initial epoch ($r_{\rm typ}$) are assumed to be from 0.01 to 1 pc. Additionally, to scrutinize dependence on ambient gas density, we consider a relatively wide range of gas density from 10^2 cm^{-3} to 10^{10} cm^{-3}. We initially set up five BHs with equal masses of 20, 25, or 30 $M_\odot$. Because of the uncertainty concerning the actual mass accretion rate, we vary the gas accretion efficiency, ϵ, in a range of 10^{-3} to 1.

We set BHs in a uniform gas sphere whose mass is 10^5 $M_\odot$. Therefore, according to the choice of gas density, the radius of gas sphere, $R_{\rm gas}$, is changed. The gas temperature is assumed to be 1000 K (therefore $c_{\rm s} = 3.709$ km s^{-1}) as in Tagawa et al. (2016). The initial positions of BHs are set randomly in a $x - y$ plane within $r_{\rm typ,}$ which is smaller than $R_{\rm gas}$. The initial velocity of each BH is given as the sum of a circular component and a random component. Circular velocity is given so that the centrifugal force should balance the gravity by gas in the $x - y$ plane. In addition, we impose random velocities in the xyz space, according to the probability of a Gaussian distribution with the same dispersion as the circular velocity.

We adjudicate that two BHs merge when their separation is less than 100 times the sum of their Schwarzschild radii. The evolution is pursued for 10 Gyr, since we consider mergers within the cosmic time. We terminate the simulation when the first BH merger occurs.

3. Models Concordant with Gravitational-wave Events

Changing the set of parameters, we have simulated 264 models, of which 135 produce a binary BH merger within 10 Gyr. We have found 16 models to match the GW events, where the final BH masses fall within the estimated mass range in the observations. In Table 1, they are listed with the assumed sets of parameters. The columns are the model number, the initial mass of BHs (m_0), the ambient gas number density ($n_{\rm gas}$), the accretion efficiency (ϵ),the initial extension of BH spatial distributions ($r_{\rm typ}$),the radius of a gaseous sphere ($R_{\rm gas}$), the final masses of merged BHs (m_1, m_2, $m_1 > m_2$), merger time ($t_{\rm merge}$), and the merger type in each run. Tagawa et al. (2016) scrutinized merger mechanisms in gas-rich environments. They found that gas dynamical friction is indispensable for BH mergers. First, the BH orbits contract due to gas dynamical friction, and then a subsequent merger is promoted through different mechanisms, which are classified into four types: a gas drag-driven merger (type A), an interplay-driven merger (type B), a three-body driven merger (type C), and an accretion-driven merger (type D).

Figure 1 demonstrates the evolution of physical quantities until the first merger in Model 3 (see Table 1 for the simulation parameters), where the (a) accretion rate, (b) mass, and (c) velocity of a heavier BH in merged BHs, and also the (d) separation of the closest pair within all BHs, are shown as a function of time. Panels (c) and (d) demonstrate that the velocity decays and that the separation of BHs shrinks owing to gas dynamical friction within 2 Myr. In this stage, the BH velocity oscillates between a subsonic and supersonic one (the sound speed being $c_{\rm s} = 3.709$ km s^{-1}), and the accretion rate intermittently reaches a super-Eddington accretion rate. In this phase, a binary forms due to energy loss by gas dynamical friction. The binary is hardened by kicking another BH through three-body interaction at around 2 Myr, which is represented by a discontinuous change of the separation. Then, the BH velocity becomes highly supersonic and therefore the accretion rate is reduced to a level much lower than an Eddington accretion rate. A component in the BH binary is sometimes replaced by another one as a result of three-body interaction. Actually, such exchange occurs at 3.7 and 5.1 Myr. Three-body interaction is repeated until 13 Myr, and eventually the binary merges into a massive BH due to GW radiation. Prior to the BH merger, the masses of merged BHs are enhanced by about ten $M_\odot$. As shown in panel (b), most of the gas accretes in an early three-body interaction phase with a subsonic velocity. Shortly before the GW emitting merger, the mass accretion rate is reduced to an Eddington accretion rate less than 10^{-5}, owing to the high circular velocity of the BH binary. In practice, the final accretion rate is dependent on the ambient gas density. In

Table 1
Sets of Parameters in which Black Holes Merged at the Masses of the Gravitational-wave Events

GW150914									
Model	m_0 ($M_\odot$)	$n_{\rm gas}$ (cm^{-3})	ϵ	$r_{\rm typ}$ (pc)	$R_{\rm gas}$ (pc)	m_1 ($M_\odot$)	m_2 ($M_\odot$)	$t_{\rm merge}$ (year)	type
1	25.0	10^3	0.1	0.1	10	37.3	28.2	3.3×10^9	C
2	25.0	10^6	0.01	0.1	1	33.3	31.3	2.8×10^7	C
3	25.0	10^7	0.01	0.01	0.46	35.8	32.3	1.3×10^7	C
4	25.0	10^8	0.01	0.01	0.22	33.8	28.7	4.2×10^5	C
5	25.0	10^{10}	0.01	0.01	0.046	34.5	32.1	5.8×10^3	C
6	30.0	10^4	0.01	1	4.6	33.3	31.2	1.0×10^9	C
7	30.0	10^4	0.01	0.1	4.6	35.6	30.8	1.0×10^9	C
8	30.0	10^4	0.01	0.01	4.6	33.4	32.0	7.7×10^8	C
9	30.0	10^5	0.01	0.1	2.2	32.4	31.2	1.5×10^8	C
10	30.0	10^6	0.01	0.1	1	34.4	32.7	9.9×10^6	C
11	30.0	10^9	0.01	0.1	0.1	34.4	32.8	1.7×10^4	C
12	30.0	10^{10}	0.001	0.01	0.046	32.1	31.9	1.2×10^4	C
GW170104									
Model	m_0 ($M_\odot$)	$n_{\rm gas}$ (cm^{-3})	ϵ	$r_{\rm typ}$ (pc)	$R_{\rm gas}$ (pc)	m_1 ($M_\odot$)	m_2 ($M_\odot$)	$t_{\rm merge}$ (year)	type
13	20.0	10^3	0.1	1	10	25.2	22.4	4.4×10^9	C
14	20.0	10^8	0.01	0.1	0.22	31.3	23.0	6.1×10^5	C
GW170814									
Model	m_0 ($M_\odot$)	$n_{\rm gas}$(cm^{-3})	ϵ	$r_{\rm typ}$ (pc)	$R_{\rm gas}$ (pc)	m_1 ($M_\odot$)	m_2 ($M_\odot$)	$t_{\rm merge}$ (year)	type
14	20.0	10^8	0.01	0.1	0.22	31.3	23.0	6.1×10^5	C
15	25.0	10^5	0.01	0.1	2.2	29.9	27.2	1.2×10^8	C
16	25.0	10^9	0.001	0.1	0.1	29.0	25.0	8.9×10^4	A

the other models listed in Table 1, the final accretion rate is $\lesssim 10^{-4}$ of the Eddington accretion rate.

In Figure 2, we plot the masses of two BHs shortly before the first mergers in 135 models out of the simulated 264 models, and compare them to the estimated mass range in the GW150914, GW170104, and GW170814 events. We find that the masses of 2 BHs are consonant to the GW150914 event in 12 models, and to the GW170104 event in 2 models, and to the GW170814 event in 3 models. Especially, Model 14 matches the GW170104 and GW170814 events, simultaneously. It worth noting that their merger types are type C (three-body driven mergers), except for Model 16 assuming extremely high-density gas. Also, it has turned out that, in these 12 models, gas of several $M_\odot$ can accrete onto BHs in early three-body interaction phases.

Abbott et al. (2016c) argued that if a strong stellar wind is assumed, a BH more massive than $25M_\odot$ should originate in a metal-free (PopIII) or ultra-low metal star. Even for a weak wind model, the progenitors should be of subsolar metal abundance. Hence, the present results imply that metal-poor stars are preferred as the progenitors of the GW150914 BHs. Figure 3 shows the accumulated mass on each BH before the merger. Since three-body interaction is a chaotic process, accreting mass in type C changes in a cataclysmic fashion. Supposing Bondi accretion, there must be uncertainties of $\sim 10M_\odot$ in accreting mass, since the merger time can fluctuate within a factor of two according to the adopted seed random number (Tagawa et al. 2015). Taking into consideration the fact that the mass uncertainties in the observations are $\sim 7M_\odot$, about a half of the models that match the masses in the GW150914 event may be missed.

As shown in Table 1, the accretion efficiency (ϵ) in the concordant models is 0.01, except for models assuming extremely high- or low-density gas (Models 1, 12, 13, and 16). Hoyle–Lyttleton-type accretion is a nonlinear function of mass, and therefore the accreting mass is a steep function of ϵ and $n_{\rm gas}$. The value of accretion efficiency is roughly determined by the balance between the accretion timescale and the merger timescale (Tagawa et al. 2016). In other words, the accumulated mass is regulated by these timescales. Actually, the timescales accord when the accretion efficiency is around 0.01.

4. Discussion

4.1. Merger Sites

We consider preferable sites for the present merger scenario. The first possibility is AGN disks, where the density is as high as $\gtrsim 10^7$ cm^{-3}, and the size is as compact as $\lesssim 1$ pc (Sirko & Goodman 2003; Burtscher et al. 2013). For a gas disk surrounding a central supermassive BH (SMBH), the Toomre Q value is estimated to be

$$Q \simeq 1.4 \left(\frac{r}{1\ {\rm pc}}\right)^{1/2} \left(\frac{M_{\rm SMBH}}{10^7\ M_\odot}\right)^{1/2} \left(\frac{M_{\rm disk}}{10^5\ M_\odot}\right)^{-1} \quad (2)$$

for disk temperature of 10^3 K, where $M_{\rm SMBH}$ and $M_{\rm disk}$ are the masses of a SMBH and an AGN disk, respectively. Hence, if $M_{\rm disk}$ is lower than $10^5\ M_\odot$, the disk is stabilized by the SMBH. However, a more massive disk should be stabilized by additional heating sources such as massive stars formed within the disk (Sirko & Goodman 2003). The viscous timescale of a disk is assessed by

$$t_{\rm vis} \simeq 10^8\ {\rm year} \left(\frac{r}{1\ {\rm pc}}\right)^{1/2} \left(\frac{\alpha}{0.1}\right)^{-1} \left(\frac{M_{\rm SMBH}}{10^7\ M_\odot}\right)^{1/2}, \quad (3)$$

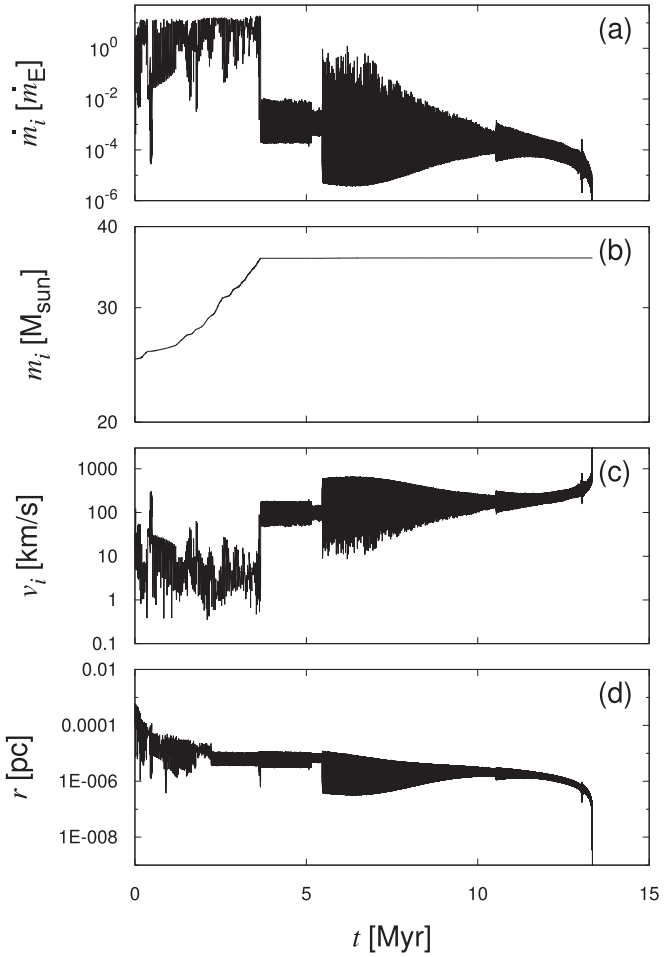

Figure 1. Time evolution of physical quantities for Model 3 in Table 1. Panels (a), (b), and (c) represent the mass accretion rate in units of the Eddington-mass accretion rate ($\dot{m}_E = L_E/c\eta$, $\eta = 0.1$), mass, and velocity for a heavier BH in merged BHs, respectively. Panel (d) shows the separation of the closest pair within all of the BHs.

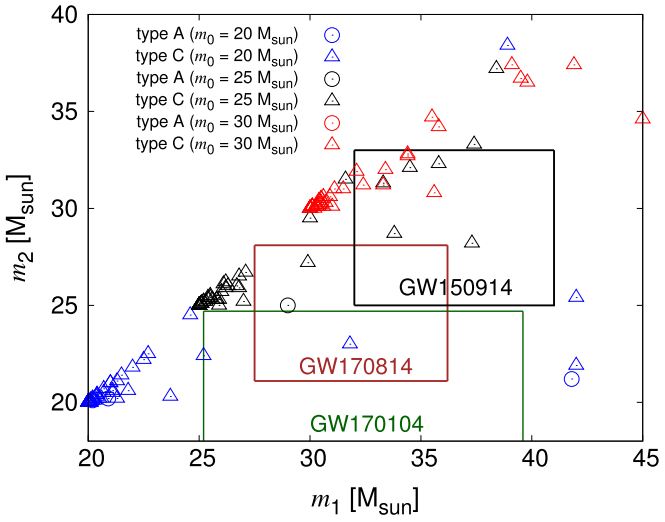

Figure 2. BH masses ($m_1 > m_2$) in a binary just before the first merger in each run. Blue, black, and red plots represent the initial masses (m_0) of 20, 25, and 30 $M_\odot$, respectively. The circles and triangles represent gas drag-driven mergers (type A) and three-body driven mergers (type C), respectively. The masses of GW150914, GW170104, and GW170814 with their uncertainties are indicated by squares.

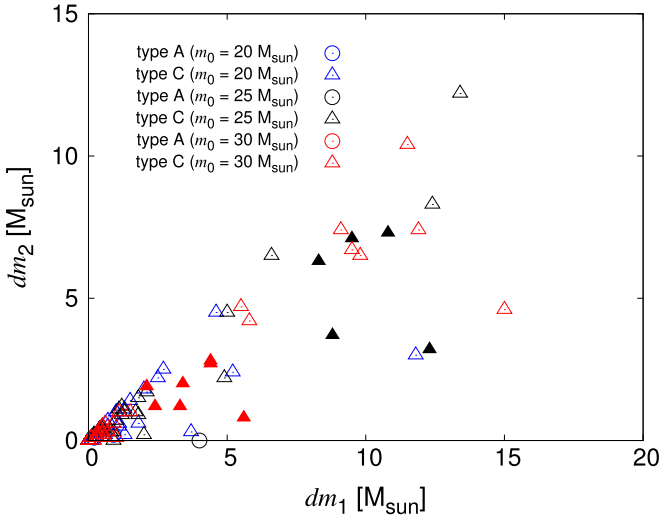

Figure 3. Same as Figure 2, but the accreted masses onto BHs before mergers are shown. The filled symbols are compatible with the GW150914 event.

where α is the standard viscosity parameter (e.g., Umemura et al. 1997), although the mass accretion may be flickering in $\sim$0.1 Myr (King & Nixon 2015). The AGN lifetime can be estimated by the duty cycle, $P_{\rm duty} = N_{\rm AGN} t_{\rm AGN}/t_{\rm H}(z)$, where $t_{\rm AGN}$ is the duration of a single AGN episode, $N_{\rm AGN}$ is the number of AGN episodes, and $t_{\rm H}(z)$ is the Hubble time at redshift z. Shankar et al. (2009) derived $P_{\rm duty}$ as a function of redshift and BH mass. For $M_{\rm SMBH} = 10^7\ M_\odot$, $P_{\rm duty} \simeq 0.03$ at $z = 0.3$ and $P_{\rm duty} \simeq 3 \times 10^{-3}$ at $z = 0$. This can be translated into $N_{\rm AGN} t_{\rm AGN} = 300$ Myr at $z = 0.3$ and 41 Myr at $z = 0$, while $N_{\rm AGN} t_{\rm AGN} = 10$ Myr at $z = 0.3$ and 1 Myr at $z = 0$ for $M_{\rm SMBH} = 10^9\ M_\odot$.

BHs whose orbits are originally misaligned with AGN disks tend to be aligned due to gas dynamical friction. The alignment timescale is estimated to be

$$t_{\rm align} = \frac{v_z^3}{12\pi G^2 m_0 m_{\rm H} n_{\rm gas}} \left(\frac{h_{\rm ini}}{h_{\rm disk}}\right) \simeq 10^8\ {\rm year} \left(\frac{h_{\rm ini}}{0.2}\right)^4 \left(\frac{h_{\rm disk}}{0.03}\right)^{-1} \left(\frac{r}{1\ {\rm pc}}\right)^{-3/2} \times \left(\frac{n_{\rm gas}}{10^7\ {\rm cm}^3}\right)^{-1} \left(\frac{m_0}{30\ M_\odot}\right)^{-1} \left(\frac{M_{\rm SMBH}}{10^7\ M_\odot}\right)^{3/2}, \quad (4)$$

where v_z is the z-component of the BH velocity, $h_{\rm disk}$ is the aspect ratio of an AGN disk (Goodman 2003), and $h_{\rm ini}$ is the aspect ratio of an initial BH orbit against an AGN mid-plane. Since $t_{\rm align}$ should be shorter than $t_{\rm AGN}$, $M_{\rm SMBH}$ is constrained to be $\lesssim 10^7\ M_\odot$. In the process of alignment, the velocity relative to the disk rotation leads to the epicyclic motion of a BH. The relative velocity decays due to dynamical friction, and simultaneously the circular orbit shrinks in the disk. When multiple BHs having residual reciprocal velocity interact with each other in the disk, the dynamics similar to the present simulations is expected. Also, the situation is analogous to the

formation of protoplanets from planetesimals in a protoplanetary disk (Kokubo & Ida 2000).[4]

Another possibility for the merger site is giant molecular clouds (GMCs). The Jeans mass of a cloud with density, $n_{\rm gas}$, and temperature, T, is $M_{\rm J} = 5 \times 10^4\ M_\odot (n_{\rm gas}/10^3\ {\rm cm}^{-3})^{-1/2} (T/10^3\ {\rm K})^{3/2}$. Therefore, if only the thermal pressure is exerted, a GMC denser than $10^3\ {\rm cm}^{-3}$ is gravitationally unstable in the free-fall time, $t_{\rm ff} = 1.6 \times 10^6\ {\rm year} (n_{\rm gas}/10^3\ {\rm cm}^{-3})^{-1/2}$. However, GMCs show large non-thermal linewidths indicating supersonic turbulence, which may prevent gravitational collapse at large scales (e.g., Boneberg et al. 2015). Actually, the lifetime of GMCs is estimated to be ~ 30 Myr, which is longer than the free-fall time (e.g., Krumholz et al. 2006).

Taking into account these timescales in the two possible sites, BH mergers should occur within 30–100 Myr. From Table 1, this condition requires $n_{\rm gas} \gtrsim 10^6\ {\rm cm}^{-3}$. Therefore, dense galactic nuclear disks and dense GMCs are potential sites for the mergers concordant with the GW events. Besides, dynamically assembled BH binaries in the present simulations predict an isotropic distribution of spin tilts without alignment with the orbital angular momentum, which is preferred to account for the misaligned spins in the GW170104 event.

4.2. Event Rate in AGNs

We estimate the event rates for mergers of massive stellar-mass BHs in the first aLIGO observation run (LIGO O1). The horizon distance of massive BH mergers is $D_h \approx 3$ Gpc ($z \approx 0.3$) (Belczynski et al. 2016), corresponding to a comoving volume of $V_c \approx 50\ {\rm Gpc}^3$. Here, we assess the event rates for massive BH mergers in AGN gas disks.

First, we consider remnant BHs of massive population I stars formed in a galaxy, say, PopI BHs. Due to inward migration of BHs by stellar dynamical friction, about $N_{\rm BH} \sim 2 \times 10^4$ BHs may exist within 1 pc from a SMBH in a Milky Way (MW)-sized Galaxy (Miralda-Escude & Gould 2000; Antonini 2014). To produce massive BHs with $\gtrsim 25\ M_\odot$, the initial progenitor mass is required to be $\gtrsim 70\ M_\odot$ (Belczynski et al. 2016). Supposing a Salpeter initial mass function with an upper mass limit of $100\ M_\odot$, $\sim 20\%$ of produced BHs are expected to be massive ($f_{\rm massive} \sim 0.2$). Hence, the fraction of massive BH pairs is $f_{\rm massive}^2 \sim 0.04$. Since the aspect ratio ($h_{\rm ini}$) represents the fraction of BHs that can align to the AGN disk, the fraction of aligned BHs in $t_{\rm AGN}$ is given by $f_{\rm align} \simeq 0.2 (t_{\rm AGN}/100\ {\rm Myr})^{1/4}$ from Equation (4). In order for a merger to take place, the condition of $t_{\rm merge} \leqslant t_{\rm AGN}$ should be satisfied, where is $t_{\rm merge} \sim 10$ Myr for $n \sim 10^7\ {\rm cm}^{-3}$ from the present simulations. Thus, it is required that $t_{\rm AGN} \geqslant 10$ Myr and therefore $N_{\rm AGN} \leqslant P_{\rm duty} t_{\rm H}(z)/10$ Myr. In the range of $M_{\rm SMBH} \leqslant 10^7\ M_\odot$ and $0 \lesssim z \lesssim 0.3$, we have $3 \times 10^{-3} \lesssim P_{\rm duty} \lesssim 3 \times 10^{-2}$ (Shankar et al. 2009). Then, $N_{\rm AGN} \leqslant 4$ at $z \sim 0$ and $N_{\rm AGN} \leqslant 31$ at $z \sim 0.3$. Using these assessments, the merger rate per MW-sized galaxy is estimated to be $\dot{N}_{\rm merge/gal} \sim P_{\rm duty} f_{\rm align} f_{\rm massive}^2 N_{\rm BH}/t_{\rm AGN} = f_{\rm align} f_{\rm massive}^2 N_{\rm BH} N_{\rm AGN}/t_{\rm H}(z) \simeq$ 10–20 ${\rm Gyr}^{-1}$ for $N_{\rm AGN} = 1$, and $\simeq$30–300 ${\rm Gyr}^{-1}$ for the maximum of $N_{\rm AGN}$. From the Schechter function fit of local galaxies, the number density of MW-sized galaxies is $n_{\rm gal} \sim 2 \times 10^6\ {\rm Gpc}^{-3}$ (Marzke et al. 1998). Using these values, the number of MW-sized galaxies involved in an observable volume is $N_{\rm gal} \sim {\rm V}_c\ n_{\rm gal} \sim 1 \times 10^8$. Under these assumptions, the event rate for mergers of massive PopI BHs in AGN disks in the first observing run of aLIGO is estimated to be $R_{\rm O1,AGN,PopI} \sim \dot{N}_{\rm merge/gal} N_{\rm gal} \simeq$ 1–2 ${\rm yr}^{-1}$ for $N_{\rm AGN} = 1$, and $\simeq$3–30 ${\rm yr}^{-1}$ for the maximum of $N_{\rm AGN}$. The volumetric event rate is $R_{\rm vol,AGN,PopI} \sim \dot{N}_{\rm merge/gal} n_{\rm gal} \simeq (2\text{–}4) \times 10^{-2}\ {\rm Gpc}^{-3}\ {\rm yr}^{-1}$ for $N_{\rm AGN} = 1$, and $\simeq$0.06–0.6 ${\rm Gpc}^{-3}\ {\rm yr}^{-1}$ for the maximum of $N_{\rm AGN}$.

Next, we consider remnant BHs of population III stars (PopIII BHs). Although there are large uncertainties, roughly 10 PopIII BHs are possibly born in a minihalo of 10^5–$10^6\ M_\odot$ (Susa et al. 2014; Valiante et al. 2016). In this case, $\sim 10^6$ PopIII BHs are expected to exist in a MW-sized galaxy (Ishiyama et al. 2016). Then, if the ratio of PopIII BHs to PopI BHs is assumed to be constant in a whole galaxy, the number of BHs in central subparsec regions is $N_{\rm BH} \sim 2 \times 10^2$. Besides, if taking into consideration the possibility that BHs within ~ 10 pc can migrate into subparsec regions, the number of BHs at $\lesssim 1$ pc can increase by about one order of magnitude (Miralda-Escude & Gould 2000). So, we suppose $N_{\rm BH} \sim 2 \times 10^3$ PopIII BHs exist in an AGN disk in a MW-sized galaxy. We assess the fraction of massive ones in all PopIII BHs to be $f_{\rm massive} \sim 0.5$ (Heger & Woosley 2002; Susa et al. 2014). Then, $\dot{N}_{\rm merge/gal} \sim P_{\rm duty} f_{\rm align} f_{\rm massive}^2 N_{\rm BH}/t_{\rm AGN} \simeq$ 6–10 ${\rm Gyr}^{-1}$ for $N_{\rm AGN} = 1$, and $\simeq$20–200 ${\rm Gyr}^{-1}$ for the maximum of $N_{\rm AGN}$. Under these assumptions, we estimate the event rate for mergers of massive PopIII BHs in AGN disks to be $R_{\rm O1,AGN,PopI} \sim \dot{N}_{\rm merge/gal} N_{\rm gal} \simeq 1\ {\rm yr}^{-1}$ for $N_{\rm AGN} = 1$, and $\simeq$ 2–20 ${\rm yr}^{-1}$ for the maximum of $N_{\rm AGN}$. The volumetric event rate is $R_{\rm vol,AGN,PopI} \sim \dot{N}_{\rm merge/gal} n_{\rm gal} \simeq 2 \times 10^{-2}\ {\rm Gpc}^{-3} {\rm yr}^{-1}$ for $N_{\rm AGN} = 1$, and $\simeq$0.04–0.4 ${\rm Gpc}^{-3}\ {\rm yr}^{-1}$ for the maximum of $N_{\rm AGN}$.

4.3. Event Rate in GMCs

Here, we estimate the event rates for BH mergers in GMCs. A MW-sized galaxy contains $\sim 10^8$ BHs in the volume of $\sim 100\ {\rm kpc}^3$ (Remillard & McClintock 2006), where the fraction of massive BHs is 0.2 as discussed in the previous section. There are ~ 1000 GMCs in a galaxy and they occupy the volume of $10^{-3}\ {\rm kpc}^3$ (Ruffle 2006). Hence, we can assume that ~ 200 massive BHs reside in GMCs. Considering that the velocity dispersion of PopI massive stars is $\sim 20\ {\rm km\ s}^{-1}$ (Binney & Merrifield 1998; Nordstrom et al. 2004) and the escape velocity of GMCs is of $\sim 10\ {\rm km\ s}^{-1}$ (Dobbs et al. 2011; Dale et al. 2012), $\sim$40% of PopI BHs can be captured by GMCs. According to probability distributions, about 3 GMCs possess more than two massive BHs. Also, the volume filling factor of dense cores in GMCs is $f_{\rm core} \sim 0.05$ (Bergin et al. 1996). Besides, stars which leave BHs more massive than $25\ M_\odot$ should be metal-poor ($\leqslant$0.3 solar metallicity) and they should be of a low-velocity dispersion (Nordstrom et al. 2004). Most of such stars exist in outer galaxies of $\gtrsim 10$ kpc (Martinez-Medina et al. 2017), where the stellar mass is $\sim$0.1 of the total galactic stellar mass. Since BHs are redistributed in the dynamical time of a galaxy, $t_{\rm dyn} \sim 100$ Myr, the merger rate in a MW-sized galaxy is $\dot{N}_{\rm merge/gal} \sim 3 \times 0.1 f_{\rm core}/t_{\rm dyn} \simeq 0.2\ {\rm Gyr}^{-1}$. Under these assumptions, the event rate for mergers of PopI BHs in GMCs is estimated to be $R_{\rm O1,GMC,PopI} \sim \dot{N}_{\rm merge/gal} N_{\rm gal} \simeq 0.02\ {\rm yr}^{-1}$ and $R_{\rm vol,GMC,PopI} \sim \dot{N}_{\rm merge/gal} n_{\rm gal} \simeq 3 \times 10^{-4}\ {\rm Gpc}^{-3}\ {\rm yr}^{-1}$.

[4] In practice, the dynamics of multiple BHs in a rotating disk should be explored in a more realistic setup, which will be done in future work.

5. Conclusions

In this paper, we have considered the mergers of unassociated BHs through a chance meeting in gas-rich environments. To elucidate the merger condition concordant with the recently detected gravitational-wave events, we have conducted highly accurate post-Newtonian *N*-body simulations on a multiple BHs system embedded in dense gas, incorporating dynamical friction, Hoyle–Lyttleton mass accretion, and general relativistic effects such as pericenter shift and gravitational-wave emission. Consequently, we have found the following:

(1) Gas dynamical friction works effectively to promote a three-body interaction of BHs in dense gas of $n_{\rm gas} \gtrsim 10^6$ cm^{-3}. Eventually, mergers are caused within 30 Myr. This scenario predicts an isotropic distribution of spin tilts, which is compatible with the spin misalignment seen in the GW170104 event.

(2) Before BH mergers, gas of several $M_\odot$ accretes onto each BH. However, gas accretion takes place predominantly during early three-body interaction phases, and the final mass accretion rates shortly before GW emmision are $\lesssim 10^{-4}$ the Eddington accretion rate. Thus, the electromagnetic counterparts of GW events might not be so luminous.

(3) We have found sets of model parameters concordant with the massive BHs detected in the GW events. In the concordant models, the initial extension of BH distributions is smaller than 1 pc. To account for the GW150914 event, the masses of seed BHs are required to be $\gtrsim 25\ M_\odot$. Hence, metal-poor stars are preferred as the progenitors of the GW150914 BHs.

(4) We have roughly estimated the event rates by the first observing run of LIGO advanced detectors. The event rates for massive PopI BHs and PopIII BHs in AGN disks are assessed to be $\simeq$1–2 yr^{-1} and $\simeq$1 yr^{-1}, respectively. If multiple episodes of AGNs are taken into consideration, the rates can be enhanced by roughly an order of magnitude. For massive PopI BHs in dense interstellar clouds, the rate is $\simeq$0.02 yr^{-1}. Hence, high-density AGN disks are a more plausible site for mergers of chance meeting BHs.

In present simulations, we have assumed a fairy simple configuration of matter. However, taking realistic situations into consideration, we should construct a more concrete model of gas distributions in a dense cloud/disk and gravitational potential, including stellar distributions and a central supermassive BH. Also, the back reaction due to gas dynamical friction may alter the BH dynamics. These effects will be explored in a future analysis.

We thank the anonymous referee for useful comments. Numerical computations and analyses were carried out on Cray XC30 and computers at the Center for Computational Astrophysics, National Astronomical Observatory of Japan, respectively. This research is also supported in part by the European Research Council under the European Unionfs Horizon 2020 Programme, ERC-2014-STG grant GalNUC 638435 and Interdisciplinary Computational Science Program in Center for Computational Sciences, University of Tsukuba, and Grant-in-Aid for Scientific Research (B) by JSPS (15H03638).

References

Abbott, B. P., Abbott, R., Abbott, T. D., et al. 2016a, PhRvL, 116, 061102
Abbott, B. P., Abbott, R., Abbott, T. D., et al. 2016b, PhRvL, 116, 241103
Abbott, B. P., Abbott, R., Abbott, T. D., et al. 2016c, ApJL, 818, L22
Abbott, B. P., Abbott, R., Abbott, T. D., et al. 2017a, PhRvL, 118, 221101
Abbott, B. P., Abbott, R., Abbott, T. D., et al. 2017b, ApJL, 851, L35
Abbott, B. P., Abbott, R., Abbott, T. D., et al. 2017c, PhRvL, 119, 141101
Antonini, F. 2014, ApJ, 794, 106
Bartos, I., Kocsis, B., Haiman, Z., & Marka, S. 2017, ApJ, 835, 165
Baruteau, C., Cuadra, J., & Lin, D. N. C. 2011, ApJ, 726, 28
Belczynski, K., Daniel, E. H., Bulik, T., & O'Shaughnessy, R. 2016, Natur, 534, 512
Bergin, E. A., Snell, R. L., & Goldsmith, P. F. 1996, ApJ, 460, 343
Binney, J., & Merrifield, M. 1998, Galactic Astronomy (Princeton, NJ: Princeton Univ. Press)
Boneberg, D. M., Dale, J. E., Girichidis, P., & Ercolano, B. 2015, MNRAS, 447, 1341
Burtscher, L., Meisenheimer, K., Tristram, K. R., et al. 2013, A&A, 558, 149
Chapon, D., Mayer, L., & Teyssier, R. 2013, MNRAS, 429, 3114
Dale, J. E., Ercolano, B., & Bonnell, I. A. 2012, MNRAS, 424, 377
de Mink, S. E., & Mandel, I. 2016, MNRAS, 460, 3545
Dobbs, C. L., Burkert, A., & Pringle, J. E. 2011, MNRAS, 417, 1318
Escala, A., Larson, R. B., Coppi, P. S., & Mardones, D. 2004, ApJ, 607, 765
Goodman, J. 2003, MNRAS, 339, 937
Hanamoto, K., Ioroi, M., & Fukue, J. 2001, PASJ, 53, 105
Heger, A., & Woosley, S. E. 2002, ApJ, 567, 532
Inayoshi, K., Haiman, Z., & Ostriker, J. P. 2016, MNRAS, 459, 3738
Ishiyama, T., Sudo, K., Yokoi, S., et al. 2016, ApJ, 826, 9
King, A., & Nixon, C. 2015, MNRAS, 453, L46
Kinugawa, T., Inayoshi, K., Hotokezaka, K., Nakauchi, D., & Nakamura, T. 2014, MNRAS, 442, 2963
Kocsis, B., Yunes, N., & Loeb, A. 2011, PhRvD, 84, 024032
Kokubo, E., & Ida, S. 2000, Icar, 143, 15
Krumholz, M. R., Matzner, C. D., & McKee, C. F. 2006, ApJ, 653, 361
Kupi, G., Amaro-Seoane, P., & Spurzem, R. 2006, MNRAS, 371, 45
Makino, J., & Aarseth, S. 1992, PASJ, 44, 141
Martinez-Medina, L. A., Pichardo, B., Peimbert, A., & Carigi, L. 2017, MNRAS, 468, 3615
Marzke, R. O., da Costa, L. N., Pellegrini, P. S., Willmer, C. N. A., & Geller, M. J. 1998, ApJ, 503, 617
McKernan, B., Ford, K. E. S., Bellovary, J., et al. 2017, arXiv:1702.07818
McKernan, B., Ford, K. E. S., Kocsis, B., Lyra, W., & Winter, L. M. 2014, MNRAS, 441, 900
McKernan, B., Ford, K. E. S., Lyra, W., & Perets, H. B. 2012, MNRAS, 425, 460
Miralda-Escude, J., & Gould, A. 2000, ApJ, 545, 847
Namekata, D., & Umemura, M. 2016, MNRAS, 460, 980
Nordstrom, B., Mayor, M., Andersen, J., et al. 2004, A&A, 418, 989
O'Leary, R. M., Kocsis, B., & Loeb, A. 2009, MNRAS, 395, 2127
Pfuhl, O., Alexander, T., Gillessen, S., et al. 2014, ApJ, 782, 101
Remillard, R. A., & McClintock, J. E. 2006, ARA&A, 44, 49
Rodriguez, C. L., Chatterjee, S., & Rasio, F. A. 2016, PhRvD, 93, 084029
Ruffle, P. 2006, PhD thesis, The Univ. Manchester
Samsing, J., MacLeod, M., & Ramirez-Ruiz, E. 2014, ApJ, 784, 71
Shankar, F., Weinberg, D. H., & Miralda-Escudé, J. 2009, ApJ, 690, 20
Sirko, E., & Goodman, J. 2003, MNRAS, 341, 501
Spitzer, L. 1978, Physical Processes in the Interstellar Medium (Princeton, NJ: Princeton Univ. Press)
Stahler, S. W. 2010, MNRAS, 402, 1758
Stone, N. C., Metzger, B. D., & Haiman, Z. 2017, MNRAS, 464, 946
Susa, H., Hasegawa, K., & Tominaga, N. 2014, ApJ, 792, 32
Tagawa, H., Kocsis, B., & Saitoh, R. T. 2018, arXiv:1802.00441
Tagawa, H., Umemura, M., & Gouda, N. 2016, MNRAS, 462, 3812
Tagawa, H., Umemura, M., Gouda, N., Yano, T., & Yamai, Y. 2015, MNRAS, 451, 2174
Umemura, M., Fukue, J., & Mineshige, S. 1997, ApJL, 479, L97
Valiante, R., Schneider, R., Volonteri, M., & Omukai, K. 2016, MNRAS, 457, 3356
Watarai, K., Fukue, J., Takeuchi, M., & Mineshige, S. 2000, PASJ, 52, 133